Agricultural and Forest Meteorology 149 (2009) 2012–2021

Contents lists available at ScienceDirect

Agricultural and Forest Meteorology

journal homepage: www.elsevier.com/locate/agrformet

Three scales of temporal resolution from automated soil respiration measurements

Kathleen Savage [a,*], Eric A. Davidson [a], Andrew D. Richardson [b], David Y. Hollinger [c]

[a] Woods Hole Research Center, 149 Woods Hole Road, Falmouth, MA 02540, United States
[b] University of New Hampshire, Complex Systems Research Center, Morse Hall, 8 College Road, Durham, NH 03824, United States
[c] USDA Forest Service, Northern Research Station, 271 Mast Road, Durham, NH 03824, United States

ARTICLE INFO

Article history:
Received 5 January 2009
Received in revised form 17 April 2009
Accepted 14 July 2009

Keywords:
Soil respiration
Coherence analysis
Diel
Synoptic

ABSTRACT

Soil respiration (R_s) is a combination of autotrophic and heterotrophic respiration, but it is often modeled as a single efflux process, influenced by environmental variables similarly across all time scales. Continued progress in understanding sources of variation in soil CO_2 efflux will require development of R_s models that incorporate environmental influences at multiple time scales. Coherence analysis, which requires high temporal frequency data on R_s and related environmental variables, permits examination of covariation between R_s and the factors that influence it at varying temporal frequencies, thus isolating the factors important at each time scale. Automated R_s measurements, along with air, soil temperature and moisture were collected at half hour intervals at a temperate forest at Harvard Forest, MA in 2003 and a boreal transition forest at the Howland Forest, ME in 2005. As in other temperate and boreal forests, seasonal variation in R_s was strongly correlated with soil temperature. The organic and mineral layer water contents were significantly related to R_s at synoptic time scales of 2–3 days to weeks, representing the wetting and drying of the soils as weather patterns move across the region. Post-wetting pulses of R_s were correlated with the amount of precipitation and the magnitude of the change from pre-wet-up moisture content to peak moisture content of the organic horizon during the precipitation events. Although soil temperature at 8–10 cm depth and R_s showed strong coherence at a 24-h interval, calculated diel Q_{10} values for R_s were unreasonably high (6–74) during all months for the evergreen forest and during the growing season for the deciduous forest, suggesting that other factors that covary with soil temperature, such as canopy assimilatory processes, may also influence the diel amplitude of R_s. Lower diel Q_{10} values were obtained based on soil temperature measured at shallower depths or with air temperature, but the fit was poorer and a lag was needed to improve the fit (peak R_s followed peak air temperature by several hours), suggesting a role for delayed substrate supply from aboveground processes to affect diel patterns of R_s. High frequency automated R_s datasets afford the opportunity to disentangle the temporal scales at which environmental factors, such as seasonal temperature and phenology, synoptic weather events and soil moisture, and diel variation in temperature and photosynthesis, affect soil respiration processes.

1. Introduction

The increasing concentrations of atmospheric carbon dioxide and other greenhouse gases are primary contributors to observed increases in global temperature. These changes are likely to alter primary productivity, autotrophic respiration, and heterotrophic respiration, and the net carbon balance of ecosystems will depend on how each of these processes responds to changes in climate (Denman et al., 2007). Soil respiration (R_s), a combination of autotrophic (root respiration, R_{root}) and heterotrophic (microbial respiration, R_{micro}) respiration, is a major carbon flux from the terrestrial biosphere to the atmosphere. R_s is primarily correlated to temperature and precipitation (via soil moisture), although there is also a growing recognition that primary productivity and substrate supply (both in terms of amount and quality) are critical drivers of R_s (Davidson et al., 2006a).

A number of studies have examined the relationship between temperature and R_s on diel and seasonal scales (Xu and Qi, 2001; Irvine and Law, 2002; Janssens and Pilegaard, 2003; Yuste et al., 2004; Gu et al., 2008). Empirical models of R_s are expressed as a scalar function of temperature, often represented by an exponential Q_{10} (van't Hoff) value (the scalar multiple by which R_s increases when temperature increases by 10 °C). However, R_s is a complex process, combining R_{micro} and R_{root}, each of which typically

* Corresponding author. Tel.: +1 508 540 9900x142; fax: +1 508 540 9700.
E-mail address: savage@whrc.org (K. Savage).

0168-1923/$ – see front matter © 2009 Elsevier B.V. All rights reserved.
doi:10.1016/j.agrformet.2009.07.008

emanates from a variety of species and which may respond differently to temperature and other covarying environmental factors such as soil water content and substrate availability (Gu et al., 2008). Responses of R_{micro} and R_{root} are also likely to differ at diel and seasonal time scales. Hence deriving one Q_{10} function representative of R_s on all time scales is overly simplistic.

In past work, when the components of R_s have been distinguished, diel responses of R_{micro} were correlated with soil temperature but R_{root} was decoupled from soil temperature and significantly related to plant phenology (Yuste et al., 2004; Tang et al., 2005a; Liu et al., 2006). R_{root} has been found to derive its carbon source from stored carbohydrates in early spring and recent photosynthate in late spring (Cisneros-Dozal et al., 2006), likely indicating new root growth in late spring. As such, diel trends in R_s during this period maybe more strongly affected by aboveground processes than soil temperature. Significant relationships have been demonstrated between R_s and leaf area index (LAI) and photosynthetically active radiation (PAR), both indicators of photosynthetic activity (Yuste et al., 2004, Liu et al., 2006). However, the time required for recently assimilated carbon to travel from leaves to roots is not well known, and studies have found both a time lag and no time lag between aboveground processes and inferred R_{root} (Davidson and Holbrook, 2009; Tang et al., 2005a; Lui et al., 2006; Gaumont-Guay et al., 2008).

The response of R_s to soil moisture is more complex and often confounded with its relationship to temperature. Soils of many temperate forests tend to dry out as evapotranspiration exceeds precipitation during summer months, thus confounding the effects of temperature on R_s (Davidson et al., 1998). Under drought conditions, water stress significantly decreases rates of R_s over weeks and months as soils gradually dry down (Savage and Davidson, 2001; Borken et al., 2006), primarily because of a decrease in R_{micro} (Cisneros-Dozal et al., 2006).

Increases in soil moisture generally result in increased R_s due to a combination of reduced microbial water stress, release of substrates from turnover of microbial biomass, and greater mobility of available substrate through soil water films (Birch, 1958; Bottner, 1985; Kieft et al., 1987; Xu et al., 2004). This response has been observed to be rapid (minutes to hours) but variable in duration (influence lasting hours to days) and magnitude (Irvine and Law, 2002; Borken et al., 2003). The magnitude and timing of pulse events can significantly influence the annual carbon budget, accounting for up to 11% of the observed seasonal flux (Lee et al., 2004; Tang et al., 2005b). The proportion of R_s derived from either R_{root} or R_{micro} differs under differing moisture conditions (Borken et al., 2006). Cisneros-Dozal et al. (2006) found that decomposition of leaf litter, an R_{micro} component of R_s, varied with moisture status, and changes in leaf litter moisture primarily drove the variability in total R_s fluxes, accounting for 1% under dry conditions and up to 42% of total R_s under wet conditions.

The objective of this study is to examine the response of R_s to changes in temperature and moisture at seasonal, diel and synoptic scales. Using high temporal frequency measurements of R_s, temperature, and moisture, we differentiate the effects of climatic variables at each temporal scale.

2. Methods

2.1. Study site

R_s was measured at the Harvard Forest near Petersham, Massachusetts USA (42°32N, 72°11W), and at the Howland Forest, near Howland Maine, USA (45°12N, 68°44W). Data presented here for Harvard Forest were collected from May 17th through November 11th, 2003, from a well drained mixed hardwood forest, approximately 70 years old. The dominant tree species is red oak. Soils are classified as Canton fine sandy loam, Typic Distrochrepts. Due to agricultural use in the 19th century, the upper mineral soil is partially disturbed. The mean annual temperature is +8.5 °C and the mean annual precipitation is 1050 mm. The precipitation total for 2003 was 1311 mm, approximately 25% greater than the annual average. See Compton and Boone (2000) and Savage and Davidson (2001) for further descriptions.

Data presented here for Howland were collected from May 4th through November 3rd, 2005, and are from a mature boreal transition forest dominated by red spruce and eastern hemlock stands that are at least 160-year old. The soils have never been cultivated and are classified as Skerry fine sandy loam, Aquic Haplorthods. The mean annual temperature is +5.5 °C, and the mean annual precipitation is 1000 mm. The precipitation total for 2005 was 1281 mm, 28% greater than the annual average. See Fernandez et al. (1993), Savage and Davidson (2001) and Hollinger et al. (2004) for further descriptions.

2.2. Automated measurements of R_s

The same automated R_s system and the same sampling strategies and protocols were used for both Harvard and Howland forests. Automated measurements of R_s were made at six chambers each of which was sampled once per half hour. For a description of the automated R_s system see Savage and Davidson (2003). Briefly, each chamber was active for a 5-min period over which time a vented chambertop would close onto the collar and a pump would circulate air from inside the chamber headspace to an infrared gas analyzer (IRGA-Licor 6252). A Campbell CR10X datalogger recorded the change in chamber headspace CO_2 concentration. Air temperature and pressure were used to correct for the number of moles of CO_2 in air. A linear regression was preformed on the increasing chamber headspace concentration to determine a flux rate. About 50,000 flux measurements were obtained for each site. A series of protocols designed to efficiently isolate suspect fluxes was utilized to analyze the data for quality (for a complete description of protocols see Savage et al., 2008). Following the data quality procedures, the final dataset for Harvard consisted of 39,876 R_s measurements and 43,673 for Howland.

2.3. Soil moisture, temperature and organic layer water content

At the Harvard Forest, soil pits were dug to a depth of 80 cm and Campbell Scientific Water Content Reflectometry probes (CS615) were installed at 4.5, 14, 36 and 61 cm. The 4.5 cm volumetric soil moisture (VSM, cm^3 H_2O cm^{-3} soil, Campbell Scientific supplied calibration equation) readings were used for subsequent analysis. Within this same pit, soil temperature was measured (type T-thermocouple) at 4.5, 8.5, 14 and 36 cm. Thirty-six DC-half bridges (for a description of DC-half bridge sensors see Borken et al., 2003) were used to measure the gravimetric water content (g H_2O g^{-1} - dry mass) of the organic layer. Briefly, the half bridge sensors are pieces of basswood (1.59 mm thick and 9 cm^2), which mimic the wetting and drying of the leaf litter. Soil temperature, organic layer water content (O_{WC}) and mineral layer VMS were measured at half hourly intervals and data were collected and stored on a Campbell Scientific CR10X datalogger.

At Howland, soil temperature was measured at 5.0, 10.0 and 20.0 depth using thermistor probes. These data we collected and maintained by the Agricultural Research Service (ARS). Data were available from ftp://130.111.198.38/DataArchives. O_{WC} was measured using 13 half bridge sensors inserted into the leaf litter layer, which consists primarily of conifer needles at Howland Forest. The VSM at the organic–mineral A interface (approximately 5–10 cm depth) was measured using Campbell Scientific Water Content

Reflectometry probes (CS616). Sampling frequency was half hourly and data were collected and stored on a Campbell Scientific CR10X.

2.4. Meteorological measurements

At Harvard, air temperature and precipitation, were measured at hourly intervals by the Harvard Forest meteorological station (http://harvardforest.fas.harvard.edu/data/p00/hf001/hf001.html). This meteorological station is located approximately 1.6 km from the study site. Photosynthetically active radiation (PAR) was measured above canopy at an eddy covariance tower located within 300 m of our site (Steve Wofsy and William Munger, Harvard University, Urbanski et al., 2007, ftp://ftp.as.harvard.edu/pub/nigec/HU_Wofsy/hf_data/).

At Howland, air temperature was measured concurrently with the automated R_s system. PAR values were collected above canopy from the main tower (ftp://epg-ftp.umaine.edu/).

2.5. Statistical analysis

Half hourly averages of the six automated R_s chambers were used for all modeling. Systat Version 10 and Microsoft Excel were used for all statistical analysis.

The model form used for the R_s and temperature relationship is the exponential Q_{10} function (Eq. (1))

$$R_s = R_{ref} Q_{10}^{(T_s-10)/10} \quad (1)$$

Models used to subsequently fit observed R_s data to temperature and moisture parameters (Eqs. (2) and (3)) are listed below. Discussion of model fit follows in Section 3.5.

$$R_s = (R_{ref} Q_{10}^{(T_s-10)/10}) \beta_1^{(O_{WC-opt}-O_{WC})^2} \quad (2)$$

$$R_s = (R_{ref} Q_{10}^{(T_s-10)/10}) \beta_1^{(O_{WC-opt}-O_{WC})^2} + a\overline{T_s}\left(\sin\left(\frac{2\pi T_d}{2400}\right) + c\right) \quad (3)$$

where T_s is half hourly soil temperature (°C), R_{ref} is R_s at 10 °C (mg C m^{-2} h^{-1}), Q_{10} is a unitless expression of the increase in R_s for each increase in 10 °C. O_{WC} is organic layer water content (g H_2O g^{-1} dry weight), β_1 modifies the shape of the quadratic fit, and $O_{WC\text{-}opt}$ is the optimal water content (g H_2O g dry weight^{-1}). $\overline{T_s}$ is mean daily soil temperature (°C, 8.5 cm for Harvard Forest and 10 cm for Howland Forest), a modifies the amplitude of the waveform, c modifies the phase of the waveform and T_d is time of day in military time.

2.6. Model fitting procedures

R_s and temperature model parameters are commonly fitted using an ordinary least squares (OLS) regression. With OLS the loss function minimizes the sum of the squared deviations. However using this method, outliers exert considerable and perhaps undue weight when fitting model parameters.

OLS and maximum likelihood optimization yield the same parameters when data errors are normally distributed and of constant variance (Press et al., 1993). R_s data error distributions for Harvard and Howland follow a double exponential, Laplace distribution, the variance of which increases with the R_s flux, and hence meet neither of the OLS assumptions (see Savage et al., 2008 for more detail). When errors violate the assumptions of a normal distribution and constant variance, then model parameters should be estimated using a maximum likelihood method. According to Press et al. (1993) this is achieved by minimizing a cost function (Ω), which is the equal to the sum, over all observations, of the absolute value of the data-model mismatch, weighted by the reciprocal of standard deviation of the estimated data error (WAD), Eq. (4);

$$\Omega = \sum_{i=1}^{n} \frac{|y_i - y_{pred}|}{\sigma(\delta i)} \quad (4)$$

where y_i is the observed flux (mg C m^{-2} h^{-1}), y_{pred} is the predicted flux (mg C m^{-2} h^{-1}), and $\sigma(\delta i)$ is a weighting function. The weighting function is based on the standard deviation of each observation measurement error (see Savage et al., 2008 for more detail). Briefly, following procedures proposed by Hollinger and Richardson (2005), a "paired observations" approach was used to infer the statistical properties of the random error, ε, from the difference, $|R_{s,t=0} - R_{s,t=24}|/\sqrt{(2)}$, between average half hourly measurements (across $n = 6$ chambers) made exactly 24 h apart, and where no precipitation event occurred during that 24 h period nor within 48 h prior. The random error was characterized by an estimate of its standard deviation, and is used as the weighting function $\sigma(\delta i)$ Eq. (5);

$$\sigma(\delta i) = 0.85 + 0.07 R_s \quad (5)$$

This error equation requires an initial predicted R_s (mg C m^{-2} h^{-1}) measurement, which was determined from the predicted R_s from the Q_{10} function in Fig. 1 (OLS fit) for both Harvard and Howland forests. Using the predicted R_s (rather than the measured R_s) allows for an uncertainty estimate that is independent of the actual error in the measured flux.

Model parameters were then optimized by minimizing Eq. (4) using the Gauss–Newton method in Systat 10. As can be seen from Fig. 1a, there is no difference in model fit between the OLS fit and WAD at the Harvard forests, however for Howland Fig. 1b, there is a difference between model fits at the warmer soil temperature range. All models used for subsequent analysis are fit using the WAD method.

Since the WAD method does not produce an R^2 value, the method developed by Richardson et al., 2006a to derive a Figure of Merit R^2 (FMR^2) value (for a detailed description of the method see Richardson et al., 2006b) was used. Briefly, a within sample null model was produced using Eq (4), (Ω_o), where y_{pred} equals the mean R_s value for the dataset. The FMR^2 is then equal to $1 - (\Omega/\Omega_o)$. The FMR^2 value from the WAD model fitting procedure can be considered similar to the multiple correlation coefficient r^2 from the OLS fitting procedure.

The 95% confidence intervals for model parameters which were fit using the WAD method, were calculated using 100 bootstrap parameter estimates (using SYSTAT 10.0) for each model (Eqs. (1)–(3)). The standard error of those 100 estimated parameters was used to determine the 95% confidence interval.

To determine if a statistically significant decrease in the Ω value occurred from one model to the next, the Ω value for 100 of the bootstrap parameters was calculated. These values were sorted and the 95th value was used to estimate the 95% confidence interval. Cost function value lower than the 95% confidence interval is considered a significant decrease in the Ω function value from one model to the next.

2.7. Coherence analysis

Coherence between two time series is akin to a correlation coefficient in the frequency domain, and is calculated as,

$$\mathrm{Coh}_{xy}(\lambda) = \frac{|f_{xy}(\lambda)|^2}{[f_{xx}(\lambda) f_{yy}(\lambda)]}$$

where $f_{xx}(\lambda)$ and $f_{yy}(\lambda)$ are the power spectra of series x and y, and $f_{xy}(\lambda)$ is the cospectrum of x and y.

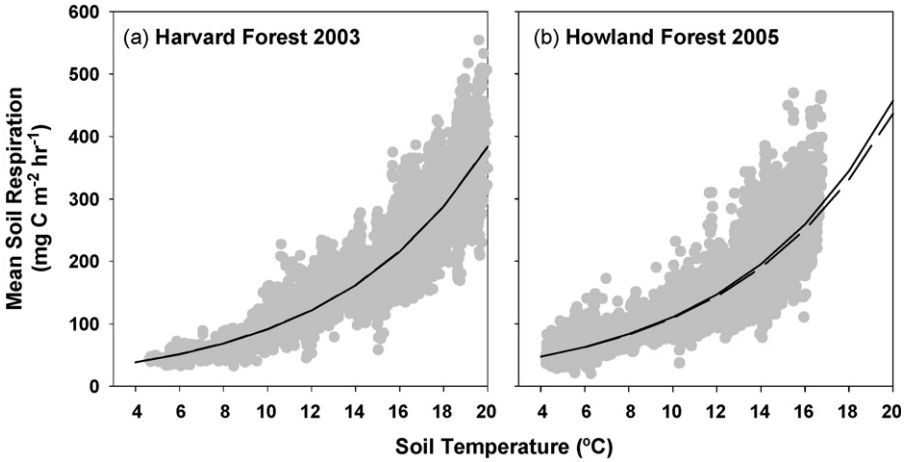

Fig. 1. (a) Harvard Forest temperature model Eq. (1), solid gray line ordinary least squares (OLS) fit, R_{ref} = 90.8, Q_{10} = 4.2; dashed line weighted absolute deviations (WAD) fit, R_{ref} = 91.3, Q_{10} = 4.2, lines overlap. (b) Howland Forest temperature model Eq. (1), solid line OLS fit, R_{ref} = 110.7, Q_{10} = 4.1, dashed gray line WAD fit, R_{ref} = 108.8, Q_{10} = 4.0.

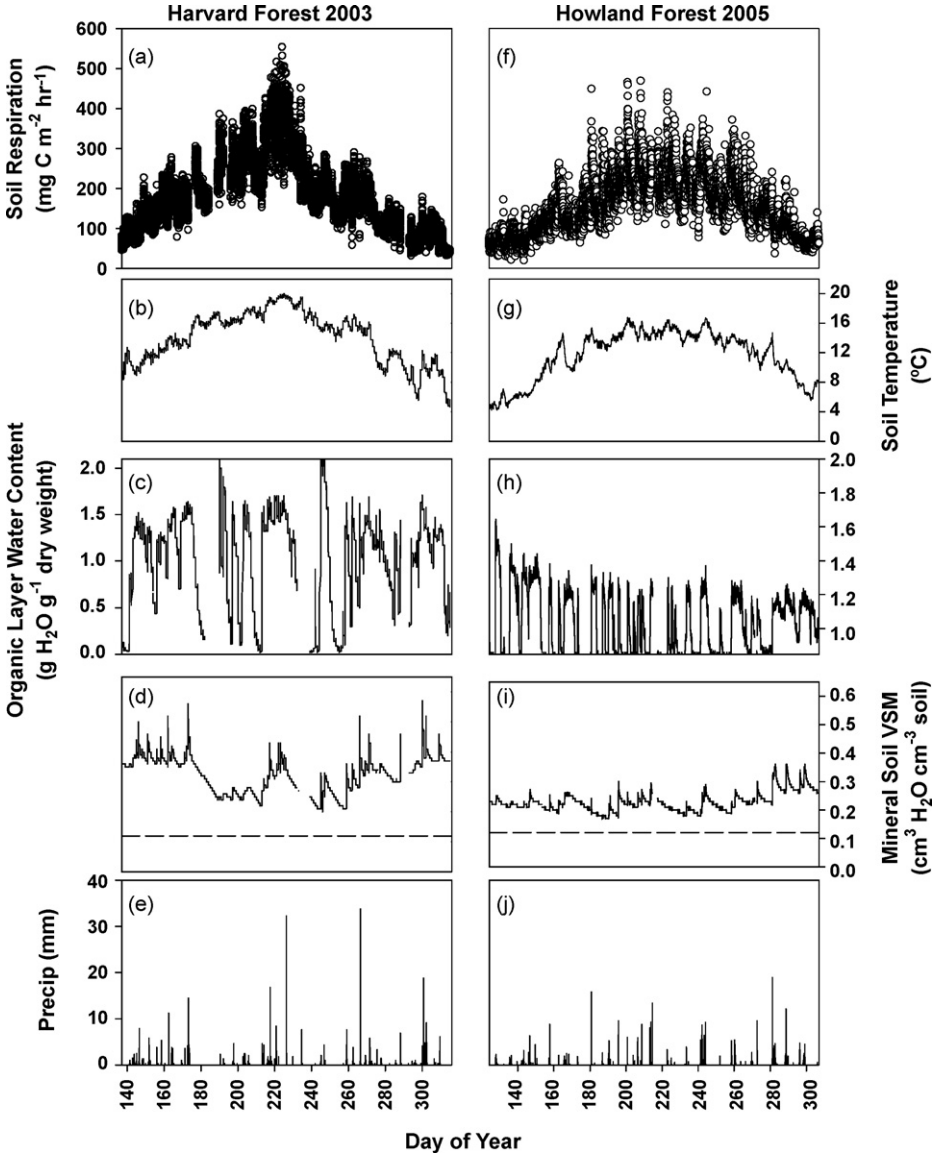

Fig. 2. (a and f) mean 1/2 hourly R_s rates, (b and c) mean 1/2 hourly soil temperature at 8.5 cm depth Harvard and 10 cm depth Howland, (c and h) mean 1/2 hourly organic layer water content (d and i) mean 1/2 hourly volumetric soil moisture content, dashed line indicated drought level (e and j) hourly precipitation.

Coherence values range from 0 (absence of any linear correlation) to 1 (perfect correlation). Time series may be coherent at some frequencies but not at others.

Using a computer program developed by Carter and Ferrie (1979) the coherence between environmental variables and R_s measurements was examined. Average R_s, temperature and moisture variables over 6 h periods were calculated to produce a continuous dataset of 512 points between the period May 18–September 22, 2003 (127 days) for Harvard, and from May 4 – September 9, 2005 (127 days) for Howland, with R_s as one time series, and either soil temperature, VSM at 4.5 cm depth or O_{WC} as the other time series.

To determine the coherence value significance level at each frequency, a Monte Carlo technique was used in which 100 artificial R_s datasets, based on a normal distribution and defined by the mean and standard deviation of the entire observed R_s dataset, were produced. The observed soil temperature was used as the independent variable for each of the 100 artificial R_s datasets for this analysis of significance. The coherence values were calculated for each of the 100 artificial datasets. Each artificial dataset was sorted with the 95th-percentile coherence values used as a threshold value of significance.

3. Results and discussion

R_s showed a strong seasonal trend, with increasing respiration as soil temperatures warm into the summer months, peaking in August, and decreasing as temperatures cool in the fall at both Harvard and Howland forests (Fig. 2a, b, f, g). R_s rates increased following precipitation events, but the magnitude and duration of those pulses varied throughout the season (Fig. 2a, c, e, f, h, j). Previous studies at these sites have demonstrated that soil moisture usually declines during the mid to late summer, with drought conditions identified when the mineral VSM decreases below 0.12 g H_2O g^{-1} soil (Savage et al., 2001). However, 2003 at the Harvard Forest and 2005 at the Howland Forest were unusually wet years, (see Section 2.1) and soil moisture in the mineral layer never fell below 0.12 g H_2O g^{-1} soil.

3.1. Coherence analysis

Coherence analysis examines the correlations between factors that influence R_s at varying temporal frequencies, enabling the isolation of those factors at time scales of interest. At both Harvard and Howland forests, R_s rates showed a significant relationship with soil temperature at a diel and seasonal frequency (Fig. 3). For synoptic weather patterns, R_s showed a significant relationship with O_{WC} and VSM at approximately 2 day and 1–2 week periods, at Harvard Forest. At Howland, R_s showed a significant relationship to VSM at 4–5 days and O_{WC} at approximately 2 and 4–7 days. The following sections address each of these temporal scales.

3.2. Seasonal scale

Air temperature and soil temperature at 4.5, 8.5, and 12 cm for the Harvard Forest and at 5, 10 and 20 cm for the Howland Forest were used to derive seasonal temperature dependence models (Eq. (1), Table 1). The figure of merit, FMR^2 (defined in Section 2.7) for the Harvard Forest model fit was best with temperature measured at 4.5 and 8.5 cm depths (FMR^2 of 0.71). For the Howland Forest the best fits were also with temperatures measured at 5 and 10 cm depths, and the FMR^2 was 0.69. Hence, for both forests, the soil temperature in the upper organic and mineral A horizons explains a large portion of the observed seasonal variation in R_s.

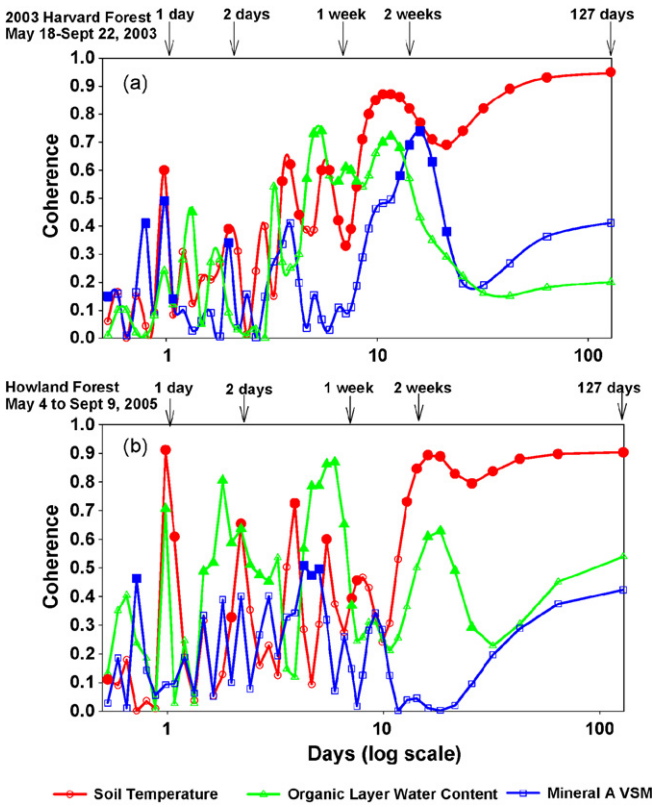

Fig. 3. Analysis of the coherence between R_s and several environmental factors, including soil temperature and moisture conditions in the organic layer and the mineral A soil, at varying time scales. VSM, volumetric soil moisture. Solid filled symbols indicated >95% significance. Harvard Forest data are presented in the upper panel; Howland Forest data in the lower panel.

3.3. Diel amplitude and pattern

The diel Q_{10} (using soil temperature at 8.5 cm for Harvard Forest and 10 cm at Howland Forest) was calculated (Eq. (1)) for periods of several days within each season that were not influenced by precipitation (either wetting up or drying down) and that contained no missing R_s measurements per day ($n = 48$ measurements per day). The calculated diel Q_{10} values were unreasonably high (from 5 to 74) for all months at the evergreen Howland Forest (Fig. 4a) and were also high (6–11) at the deciduous Harvard Forest (Fig. 4b) during months when leaves were present. High Q_{10} values (>3) have been interpreted as an indicator that factors other than temperature, but that covary with temperature, also contribute to temporal variation in soil respiration (Davidson et al., 2006a). The

Table 1
Results from fitting Eq. (1) using different soil temperature depths and air temperature. Half widths of 95% confidence intervals presented in *(italics)*. FMR^2 defined in Section 2.7.

	R_{ref}	Q_{10}	FMR^2
Harvard Forest			
Air temperature	109.4 (*0.10*)	1.8 (*0.002*)	0.47
Soil temperature at 4.5 cm	94.2 (*0.08*)	3.7 (*0.006*)	0.71
Soil temperature at 8.5 cm	91.3 (*0.08*)	4.2 (*0.008*)	0.71
Soil temperature at 12 cm	89.5 (*0.08*)	4.2 (*0.006*)	0.70
Soil temperature at 36 cm	90.5 (*0.16*)	5.6 (*0.02*)	0.51
Howland Forest			
Air temperature	98.6 (*0.13*)	1.6 (*0.001*)	0.36
Soil temperature at 5 cm	104.7 (*0.06*)	3.6 (*0.005*)	0.69
Soil temperature at 10 cm	108.7 (*0.08*)	4.0 (*0.007*)	0.69
Soil temperature at 20 cm	110.7 (*0.08*)	4.3 (*0.01*)	0.64
Soil temperature at 50 cm	127.1 (*0.11*)	4.1 (*0.01*)	0.52

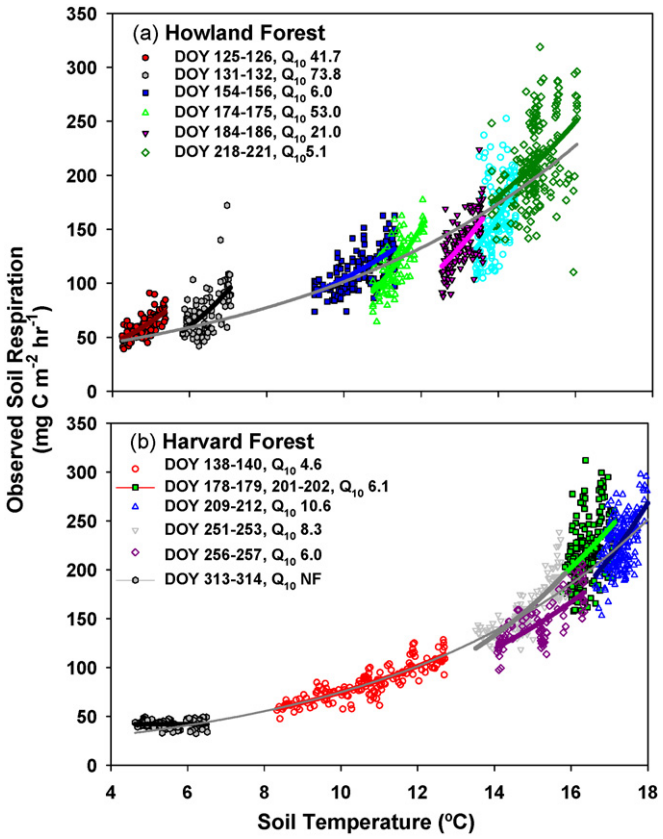

Fig. 4. Diel Q_{10} fits (Eq. (1)) of sections of data from Harvard and Howland Forest. Q_{10} values follow the legend symbols for day of year (DOY). All models are significant $p < 0.0001$. Thin dark gray line is the Q_{10} (4.5 Harvard Forest, 3.8 Howland Forest) fit using the above sets of R_s and soil temperature data.

seasonal Q_{10} of about four reported in this study (Fig. 1) suggests that the phenology of seasonal C inputs to the soil may covary with temperature. Similarly, the very high diel Q_{10} values (>6) when a canopy was present indicate that processes other than the direct effects of varying soil temperature must be influencing the diel amplitude of R_s during seasons when photosynthesis occurs. The most likely explanation is that substrate supply for root respiration probably covaries with both seasonal and diel soil temperature variation and contributes to the seasonal and diel amplitudes. Gaumont-Guay et al. (2006) also reported that hourly R_s peaked 3–5 h after soil temperature (measured at 2 cm depth) peaked in a boreal aspen forest, and they similarly inferred a delayed response to aboveground processes. However, in contrast to our results, they reported that diel Q_{10} values were lower than seasonal Q_{10} values, probably because soil moisture was a strong limiting factor during the middle and late parts of the growing season in their boreal forest, which dampened the observed response of R_s to diel variation in soil temperature.

Because the depth of soil temperature measurement clearly affects the calculated Q_{10}, we also derived diel temperature functions using measurements at shallower soil depths and air temperature (Table 1). We then compared predicted R_s for each temperature function with hourly average estimates of observed R_s (Fig. 5). At both sites, predicted R_s based on air temperature greatly over-predicted observed diel amplitudes, and the estimated peak preceded observed R_s peaks by several hours. The predicted R_s using the 4.5–5 cm depths and observed R_s showed similar diel amplitudes, but the estimated peak R_s preceded observed peak R_s by 3–4 h. The predicted diel amplitude of R_s from the 8.5–10 cm temperature function under-predicts observed R_s amplitude, but the peaks generally occurred at the same times. In summary, using temperatures measured at 4–5 cm depths, the correct diel amplitude can be simulated, but with the wrong timing of the peak, whereas using temperatures measured at 8–10 cm provides a better fit of the temporal pattern but under-predicts the amplitude.

Our previous estimates of CO_2 production as a function of depth within the Harvard Forest soil profile (Davidson et al., 2006c) indicate that only about one-third of the CO_2 production occurs in the B and C horizons, which means that deep soil CO_2 production is unlikely to explain a large delayed peak in soil CO_2 efflux. A more likely explanation is that soil temperature measured at 4.5–5 cm depth, which is at or below where most of the CO_2 is produced, provides a good estimate of diel variation of total soil CO_2 production, but that a lag of several hours is needed to account for the time necessary for photosynthate and/or a plant signal to move down the phloem to roots to affect the root respiration component of R_s. However, knowledge of probable time lags between above and belowground processes is virtually nonexistent for most plants and especially for forest ecosystems (Davidson and Holbrook, 2009; Thompson and Holbrook, 2004; Gaumont-Guay et al., 2008).

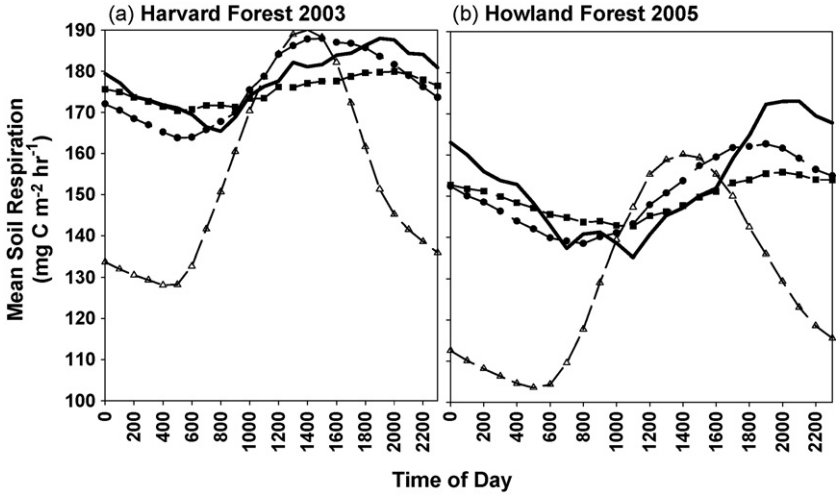

Fig. 5. Diel average R_s. Thick black line is observed diel average. Closed circles are predicted using soil temperate at 4.5 (Harvard) and 5.0 (Howland) cm depth. Closed squares are predicted using soil temperature at 8.5 cm (Harvard) and 10.0 cm (Howland). Open triangles are predicted using air temperature. Q_{10} values for each predicted model from Table 1.

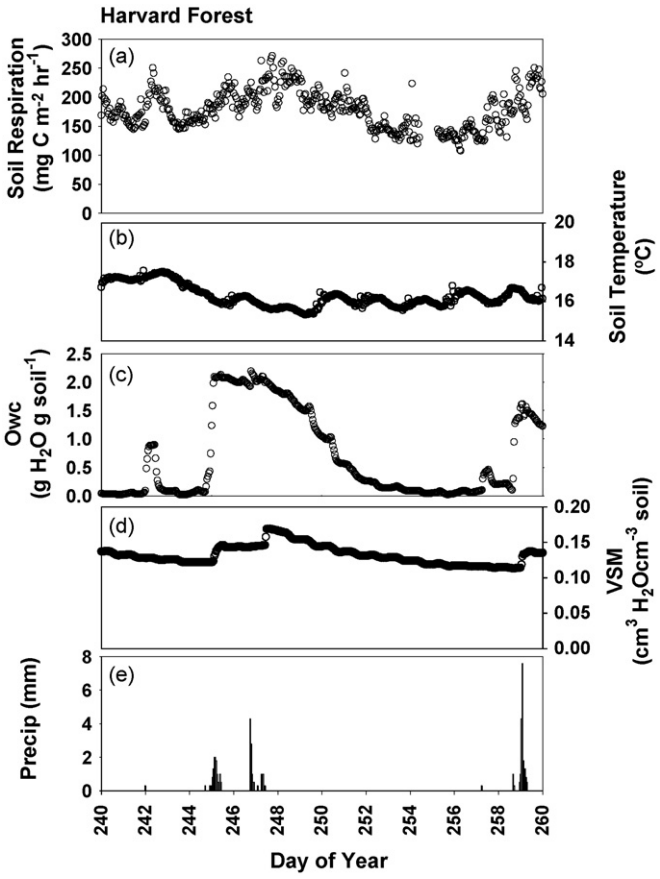

Fig. 6. R_s response to wet-up events. VSM is volumetric soil moisture.

The diel pattern of R_s also has implications for calculations of total ecosystem respiration (TER). In studies of net ecosystem exchange of CO_2 using tower based eddy covariance, TER can be measured only at night, when photosynthesis is not active. To calculate daytime TER, a Q_{10} function derived from nighttime measurements of TER and air or soil temperature is often used to predict daytime TER values based on daytime air or soil temperatures. Hence, daytime TER is assumed to exceed measured nighttime TER. However, our measurements of R_s at both Harvard and Howland forests demonstrate that R_s peaked after sunset, after both air and soil temperatures begin to decline. Observed seasonal average nighttime R_s values exceeded daytime values at the Harvard Forest (nighttime mean 184, and STErr 1.7, daytime mean 181 and STErr 1.3 mg C m^{-2} h^{-1}) and particularly at Howland (nighttime mean 164, and STErr 1.31, daytime mean 147 and STErr 0.92 mg C m^{-2} h^{-1}). Because R_s is 60–80% of TER in these forests (Davidson et al., 2006b; Goulden et al., 1996), TER may be as high or higher after sunset than during the day and is unlikely to be accurately predicted by a Q_{10} function based on daytime air temperatures. Although the differences between night and day estimates of R_s shown here are small, they are in the opposite direction from the assumption that daytime TER should be higher than nighttime TER based on adjusting measured nighttime TER with a temperature function to estimate daytime TER. The cumulative effect of even modest over-prediction of daily daytime TER could significantly affect estimates of annual TER and gross primary productivity (Gaumont-Guay et al., 2006).

3.4. Synoptic scale

The coherence analysis showed a significant relationship between R_s and O_{WC} and VSM content at 2 day and 1–2 week intervals, consistent with the movement of synoptic weather patterns across the area, causing the litter and soil layers to wet and dry. R_s was responsive to even small events that wetted only the organic layer (Fig. 6a and c Harvard). As the litter layer dried, R_s began to decrease (Fig. 6a and c). These wet-up responses to precipitation events are also evident at Howland, although they are not as dramatic as at Harvard. Pulse release of CO_2 efflux during and following precipitation events has been observed in many studies (Borken et al., 2003; Xu et al., 2004; Tang et al., 2005b; Cisneros-Dozal et al., 2006). Desiccation stress causes some microbial death, which then provides readily available substrate that the remaining living microbes can efficiently and quickly utilize once it becomes mobile with increased water content, often called the Birch effect, (Birch, 1958; Bottner, 1985; Kieft et al., 1987).

To further investigate the link between wetting and drying patterns, the relationship between R_s and wet-up events was examined at Harvard. To establish a baseline R_s which is not influenced by precipitation, data were filtered for only observed R_s measured >48 h from a precipitation event. Using this "dry R_s" dataset, a Q_{10} model of dry R_s and soil temperature at 10 cm depth (R_{ref} = 81.69 mg C m^{-2} h^{-1}, Q_{10} = 3.6) was developed. Dry R_s for DOY 137–315 estimated from this Q_{10} function were used as the baseline R_s (Fig. 7, solid black line). Visual inspection of the data both pre and post precipitation events showed that once O_{WC} content dropped below ~1 g H_2O g^{-1} dry weight, R_s declined steadily. Therefore, a precipitation event was defined as the period from the beginning of rainfall until the point when O_{WC} fell below 1 g H_2O g^{-1} dry weight. Fig. 7 shows an example section of the dataset to demonstrate this method. The light gray areas represent the proportion of the flux estimated to have been stimulated by precipitation, which is the summed difference between observed R_s and the baseline dry R_s. The total R_s for the 20 measured events at the Harvard Forest was 452 g C m^{-2}. The sum of the difference between observed R_s and dry R_s for these 20 periods totaled 55 g C m^{-2}, representing an increase of 12% in R_s due to the effects of the precipitation during the measurement period (55 g C m^{-2}/452 g C m^{-2}) and 8% of the total seasonal flux (55 g C m^{-2} total flux due to wet-up response/703 g C m^{-2} total seasonal flux).

The increase in R_s attributed to each precipitation event was significantly correlated to the total precipitation during the events and to the change in O_{WC} from pre-wetting to the maximum O_{WC} during the event (Fig. 8). The magnitude of the response of R_s to a precipitation event was greatest when the O_{WC} was very dry prior

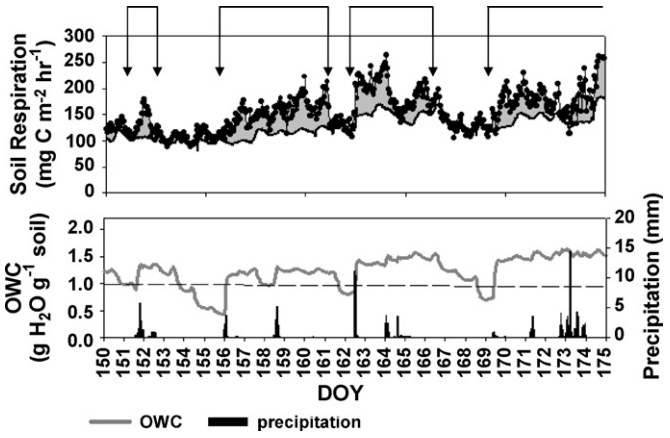

Fig. 7. R_s measurements corresponding to wet-up event. Solid circles are observed R_s, solid thick black line is predicted "dry" R_s. Gray shaded area denotes R_s response to a wet-up event. A wet-up event begins with the start of precipitation and ends when leaf litter water content dips below 1 g H_2O g^{-1} dry weight (dashed line). Arrows shows four examples of the start and end of wet-up responses.

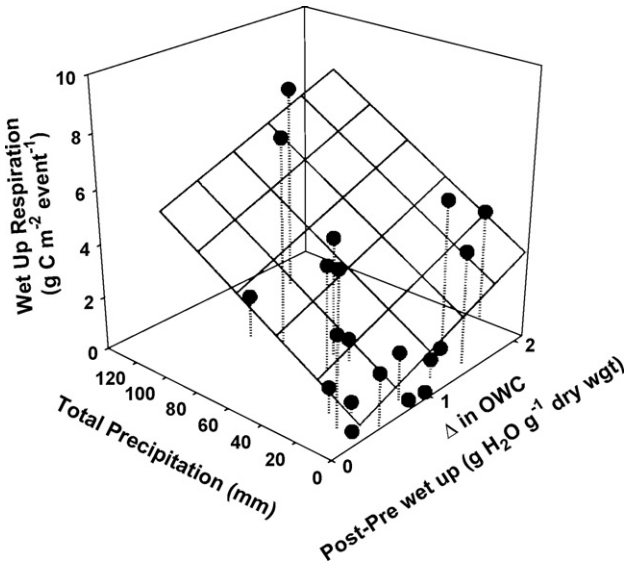

Fig. 8. Relationships between the post-wetting response of R_s and the total amount of respiration and the change in water content of the organic horizon. The relationship between wet-up SR and total precipitation ($R^2 = 0.36$, $p = 0.005$), and wet-up SR and ΔO_{WC} ($R^2 = 0.12$, $p = 0.07$). For the above fitted surface is: Wet-up $R_s = 1524 \times \Delta$organic $H_2O + 39 \times P$, $R^2 = 0.45$, $p = 0.001$, Δ in O_{WC} is defined as the difference between O_{WC} before the precipitation event and the maximum O_{WC} during the precipitation event.

to wet-up. Large precipitation events yielded a bigger pulse because they sustained elevated O_{WC} longer. Hence, total precipitation and the change in O_{WC} were found to be good predictors of the magnitude of the wet-up response.

3.5. Integrating empirical models at seasonal, synoptic and diel scales

Based on the identification of three important temporal scales of variation in the coherence analysis (Fig. 3), empirical models for R_s were developed using environmental variables representing processes at each temporal scale. First, the seasonal Q_{10} functions (Eq. (1)) based on soil temperature measured in the A horizon explain most of the variation in observed R_s (Table 2). This seasonal relationship with soil temperature is likely a combination of the influence of both R_{root} and R_{micro}. As soil temperatures warm from spring to summer, both microbial activity and primary productivity increase with soil temperature, and then fall off in autumn when temperatures begin to decline.

Second, because the organic water content affected R_s at synoptic scales, an equation that modified the R_s response as the organic layer water content wets and dries due to precipitation events was used (Eq. (2)). Visual inspection of the residuals from Eq. (1) in relation to O_{WC} showed maximum positive residuals at O_{WC} values of 1.5 and 1.2 g H_2O g dry weight^{-1}, for the Harvard and Howland forests, respectively, which were adopted as the values for O_{WC}-opt in Eq. (2). The residuals generally declined at O_{WC} values above and below O_{WC}-opt, and the shape of this curve was determined by fitting the parameter β_1 in Eq. (2). The model fit using this O_{WC} function in Eq. (2) increased FMR^2 from 0.71 (Eq. (1)) to 0.76 for the Harvard Forest (Table 2). At Howland Forest, the range of O_{WC} values is smaller and the influence of O_{WC} on observed R_s is less obvious than at Harvard. Measured O_{WC} rarely exceeds the optimal water content ($O_{WC} = 1.2$ g H_2O g soil^{-1}) at Howland Forest, and the addition of O_{WC} to the model only slightly improved model fit (Table 2). The model also fails to capture the effects of wetting events on R_s at Howland (Fig. 9b) as well as it does for Harvard (Fig. 9a). We speculate that the DC-half bridges used to estimate O_{WC} may not reflect variation in water content of the predominantly spruce and hemlock litter at Howland Forest as well as in the predominantly hardwood litter layer at Harvard Forest. The needle litter may dry and re-wet more abruptly than do the basswood pieces used in the DC-half bridges. For each forest, wetting and drying of the litter layer probably has a dominant effect on R_{micro} (Borken et al., 2006; Cisneros-Dozal et al., 2006).

Third, a sine wave function was used to amplify the diel trend in R_s beyond that predicted from half hourly soil temperature alone (Eq. (1)). We found that the daily amplitude of R_s was correlated with mean daily soil temperature:

$$\mathrm{Da} = 10.7\exp^{(0.15\overline{T_s})}, \quad R^2 = 0.51,\ p < 0.0001$$

where Da is daily amplitude (mg C m^{-2} h^{-1}), $\overline{T_s}$ mean daily soil temperature (°C)

In other words, as the daily flux of R_s increases with soil temperature, the diel amplitude of R_s also increases, but this increase in amplitude exceeds that which would be expected by the diel amplitude of hourly soil temperature. Hence, an additional predictor of daily amplitude, mean daily soil temperature ($\overline{T_s}$) is needed, as shown in Eq. (3).

Adding this diel response, (Eq. (3)) decreases the cost function Ω, and improved the model, more so for Howland than for Harvard (Table 2, Fig. 9). Some diel variation in R_s is predicted by variation in soil temperature in Eq. (1), but as discussed above, hourly variation in soil temperature alone under-predicts the diel variation. The large diel variations in R_s and the extremely high diel Q_{10} response of R_s to soil temperature (Fig. 4) during the warm season cannot be explained by a reasonable response to diel variation in soil temperature alone, suggesting a link to other process, such as allocation and lagged transport of photosynthate to roots at diel time scales. Seasonal variation in mean daily temperature is probably serving as a proxy in this case for seasonal variation in canopy processes, including mean daily NPP and subsequent belowground C allocation, thus offering a viable explanation that links canopy and belowground processes. Interestingly, the unusually high Q_{10} values derived for diel variation in R_s were not found when the canopy was absent during the leafless season of the deciduous Harvard Forest (Fig. 4).

We investigated correlations between metrics of photosynthetically active radiation (PAR) and the seasonal trend of variation in

Table 2
Model parameters for Harvard and Howland Forest and half widths of 95% confidence intervals presented in *(italics)*. Optimal O_{WC} for Harvard was set to 1.5 g H_2O g dry weight^{-1} and Howland was 1.2 g H_2O g dry weight^{-1}. FMR^2 and Ω defined in Section 2.7.

	R_{ref}	Q_{10}	β_1	a	c	Ω	FMR^2
Harvard 2003							
Eq. (1)	91.3 (*0.08*)	4.2 (*0.008*)				13,905	0.71
Eq. (2)	97.8 (*0.06*)	4.2 (*0.006*)	0.87 (*0.0006*)			11,490	0.76
Eq. (3)	97.9 (*0.08*)	4.2 (*0.006*)	0.86 (*0.0006*)	0.32 (*0.008*)	2.66 (*0.02*)	11,396	0.76
Howland 2005							
Eq. (1)	108.7 (*0.08*)	4.0 (*0.007*)				17,047	0.69
Eq. (2)	114.4 (*0.09*)	4.2 (*0.009*)	0.41 (*0.004*)			16,530	0.70
Eq. (3)	115.6 (*0.10*)	4.2 (*0.008*)	0.37 (*0.004*)	0.79 (*0.008*)	2.47 (*0.01*)	16,036	0.71

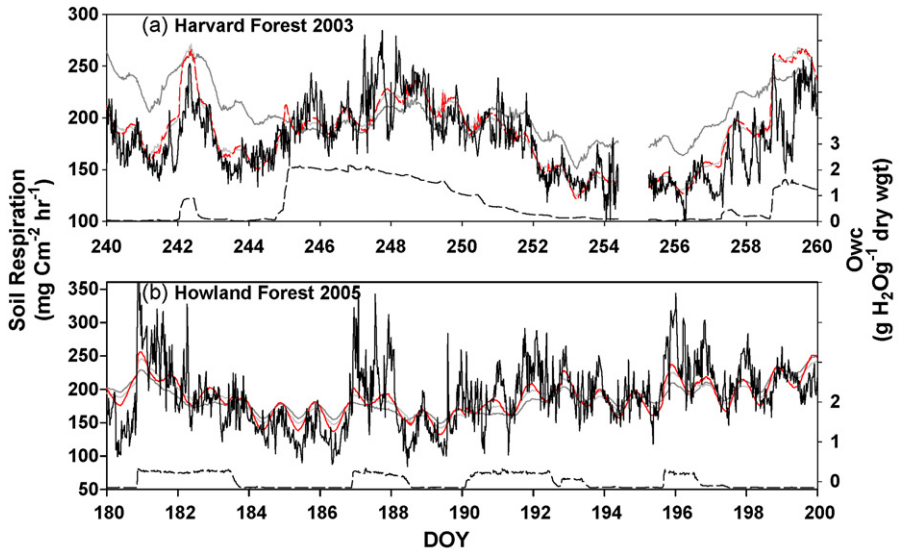

Fig. 9. Sections of observed R_s with model results for (a) Harvard, (b) Howland. Black line observed soil respiration, dark light gray line Eq. (1), light gray line Eq. (2), red line Eq. (3), and dashed black line O_{WC}. (For interpretation of the references to color in this figure legend, the reader is referred to the web version of the article.).

daily amplitude of R_s, but variation in PAR is also confounded with incidence of precipitation events. After filtering out R_s data affected by precipitation, a significant seasonal correlation between PAR and daily amplitude of R_s was not present in the remaining (n = 26 for Harvard Forest and n = 25 days for Howland Forest) dataset. The same problem complicated the use of eddy-covariance measurements of net ecosystem exchange (NEE) or gross primary productivity (GPP) as predictors of daily amplitude of R_s. Using GPP has the additional problem that it is a derived term that requires estimates of ecosystem respiration, of which R_s is typically about 60–80%. Hence, a correlation between GPP and R_s would only serve to reinforce that R_s is a large part of estimated GPP and could not be used to deduce that variation in estimated GPP drives variation in R_s, even though that may indeed be the case if GPP could be measured independently.

4. Conclusions and future directions

A single soil temperature function has often been used as a predictor of R_s at both diel and seasonal timescales. However, diel variation in R_s exceeded predicted values based on a seasonal soil temperature function. Some of the diel variation observed in R_s may be related to diel variation in aboveground processes, possibly affecting the R_{root} contribution to R_s. It is difficult to measure changes in substrate supply, particularly at a diel time scale. However these and other results suggest that substrate supply must be addressed at multiple time scales. A key gap in our knowledge is the time required and the processes involved in allocation and transport of photosynthate belowground, which affects the timing and magnitude of variation of root respiration.

Another complex process is the response of R_s to changes in soil water content. This response has been found to covary with temperature, duration and magnitude of precipitation, and with pre-wet-up conditions, something not completely addressed in the statistical models presented here or elsewhere. Hence both the antecedent conditions and the magnitude of the event are important.

In this study, we deconstructed R_s into differing temporal frequencies and then related R_s responses at each temporal frequency to the environmental variables that covaried with R_s at that scale of interest. However, these multiple factors are difficult to include in purely statistical models. Our statistical approach provides insight into the processes most important at each temporal scale, but future progress in modeling R_s will need to represent mechanisms for the processes that statistical models identify as important at each appropriate temporal scale.

Acknowledgements

The authors would like to thank Holly Hughes for all her efforts at Howland Forest. We also thank the Northeast Wilderness Trust and GMO, LLC for providing access to the research site in Howland, Maine. This research was supported by the Office of Science (BER), U.S. Department of Energy, Interagency Agreement no. DE-AI02-07ER64355, and by the U.S. Department of Energy's Office of Science (BER) grants nos. 07-DG-11242300-091 and DE-FG02-00ER63002, and through the Northeastern Regional Center of the National Institute for Climatic Change Research, grant no. DE-FC02-06ER64157.

References

Birch, H.F., 1958. The effects of soil drying on humus decomposition and nitrogen availability. Plant and Soil 10, 9–31.
Borken, W., Davidson, E., Savage, K., Gaudinski, J., Trumbore, S., 2003. Drying and wetting effects on carbon dioxide release from organic horizons. Soil Science Society of America Journal 67, 1–9.
Borken, W., Savage, K., Davidson, E., Trumbore, S., 2006. Effects of experimental drought on soil respiration and radiocarbon efflux from a temperate forest soil. Global Change Biology 11, 1–17.
Bottner, P., 1985. Response of microbial biomass to alternate moist and dry conditions in a soil incubated with ^{14}C- and ^{15}N-labelled plant material. Soil Biology and Biochemistry 17, 329–337.
Carter, G.C., Ferrie, J.F., 1979. A Coherence Spectral Estimation Program. Weinstein, C.J. (Programs for digital signal processing), 2. 3-1-2. 3-18. IEEE Press, New York.
Cisneros-Dozal, L.M., Trumbore, S., Hanson, P.J., 2006. Partitioning sources of soil-respired CO_2 and their seasonal variation using a unique radiocarbon tracer. Global Change Biology 12, 194–204.
Compton, J.E., Boone, R.D., 2000. Long-term impacts of agriculture on organic matter pools and nitrogen transformation in central New England forests. Ecology 81, 2314–2330.
Davidson, E.A., Holbrook, N.M., 2009. Is temporal variation of soil respiration linked to the phenology of photosynthesis? In: Noormets, A. (Ed.), Phenology of Ecosystem Processes: Applications in Global Change Research. Springer, New York.
Davidson, E., Belk, E., Boone, R., 1998. Soil water content and temperature as independent or confounded factors controlling soil respiration in a temperate mixed hardwood forest. Global Change Biology 4, 217–227.
Davidson, E., Janssens, I.J., Luo, Y., 2006a. On the variability of respiration in terrestrial ecosystems: moving beyond Q_{10}. Global Change Biology 12, 154–164.
Davidson, E.A., Richardson, A.D., Savage, K.E., Hollinger, D.Y., 2006b. A distinct seasonal pattern of the ratio of soil respiration to total ecosystem respiration in a spruce-dominated forest. Global Change Biology 12, 230–239.

Davidson, E.A., Savage, K., Trumbore, S.E., Borken, W., 2006c. Vertical partitioning of CO_2 production within a temperate forest soil. Global Change Biology 12, 944–956.

Denman, K.L., Brasseur, G., Chidthaisong, A., Ciais, P., Cox, P.M., Dickinson, R.E., Hauglustaine, D., Heinze, C., Holland, E., Jacob, D., Lohmann, U., Ramachandran, S., da Silva Dias, P.L., Wofsy, S.C., Zhang, X., 2007. Couplings between changes in the climate system and biogeochemistry. In: Solomon, S., Qin, D., Manning, M., Chen, Z., Marquis, M., Averyt, K.B., Tignor, M., Miller, H.L. (Eds.), Climate Change 2007: The Physical Science Basis. Contribution of I to the Fourth Assessment Report of the Intergovernmental Panel on Climate Change. Cambridge University Press, Cambridge, United Kingdom; New York, NY, USA.

Fernandez, I.J., Rustad, L.E., Lawrence, G.B., 1993. Estimating total soil mass, nutrient content and trace metals in soils under a low elevation spruce-fir forest. Canadian Journal of Soil Science 73, 317–328.

Gaumont-Guay, D., Black, T.A., Griffis, T.J., Barr, A.G., Jassal, R.S., Nesic, Z., 2006. Interpreting the dependence of soil respiration on soil temperature and water content in a boreal aspen stand. Agricultural and Forest Meteorology 140, 220–235.

Gaumont-Guay, D., Black, T.A., Barr, A.G., Jassal, R.S., Nesic, Z., 2008. Biophysical controls on rhizospheric and heterotrophic components of soil respiration in a boreal black spruce stand. Tree Physiology 28, 161–171.

Goulden, M., Munger, J., Fan, S.-M., Daube, B., Wofsy, S., 1996. Exchange of carbon dioxide by a deciduous forest: response to interannual climate variability. Science 271, 1576–1578.

Gu, L., Hanson, P.J., Post, W.M., Liu, Q., 2008. A novel approach for identifying the true temperature sensitivity from soil respiration measurements. Global Biogeochemical Cycles 22, GB4009, doi:10.1029/2007GB003164.

Hollinger, D., Richardson, A.D., 2005. Uncertainty in eddy covariance measurements and its application to physiological models. Tree Physiology 25, 873–885.

Hollinger, D.Y., Aber, J., Dail, B., Davidson, E.A., Goltz, S.M., Hughes, H., Leclerc, M.Y., Lee, J.T., Richardson, A.D., Rodrigues, C., Scott, N.A., Achuatavarier, D., Walsh, J., 2004. Spatial and temporal variability in forest–atmosphere CO_2 exchange. Global Change Biology 10, 1–18.

Irvine, J., Law, B., 2002. Contrasting soil respiration in a young and old-growth ponderosa pine forest. Global Change Biology 8, 1183–1194.

Janssens, I., Pilegaard, K., 2003. Large seasonal changes in Q_{10} of soil respiration in a beech forest. Global Change Biology 9, 911–918.

Kieft, T.L., Soroker, E., Firestone, M.K., 1987. Microbial biomass response to a rapid increase in water potential when dry soil is wetted. Soil Biology and Biochemistry 19, 119–126.

Lee, X., Wu, H.-J., Sigler, J., Oishi, C., Siccama, T., 2004. Rapid and transient response of soil respiration to rain. Global Change Biology 10, 1017–1026.

Liu, Q., Edwards, N., Post, W., Gu, L., Ledford, J., Lenhart, S., 2006. Temperature-independent diel variation in soil respiration observed from a temperate deciduous forest. Global Change Biology 12, 2136–2145.

Press, W.H., Teukolsky, S.A., Vetterling, W.T., Flannery, B.P., 1993. Numerical Recipes in Fortran 77: The Art of Scientific Computation. Cambridge University Press, New York.

Richardson, A., Braswell, D., Hollinger, B., Burman, D., Davidson, P., Evans, E., Flanagan, R., Munger, L., Savage, W., Urbanski, K., Wofsy, S., 2006a. Comparing simple respiration models for eddy flux and dynamic chamber data. Agricultural and Forest Meteorology 141, 219–234.

Richardson, A.D., Hollinger, D., Gurba, G., Davis, K., Flanagan, L., Katul, G., Munger, J., Ricciuto, D., Stoy, P., Suyker, A., Verma, S., Wofsy, S., 2006b. A multi-site analysis of random error in tower-based measurements of carbon and energy fluxes. Agricultural and Forest Meteorology 136, 1–18.

Savage, K., Davidson, E., 2001. Interannual variation of soil respiration in two New England forests. Global Biogeochemical Cycles 15, 337–350.

Savage, K., Davidson, E., 2003. A comparison of manual and automated systems for soil CO_2 flux measurements: trade-offs between spatial and temporal resolution. Journal of Experimental Botany 54, 891–899.

Savage, K., Davidson, E., Richardson, A.D., 2008. A conceptual and practical approach to data quality and analysis procedures for high-frequency soil respiration measurements. Functional Ecology 22, 1000–1007.

Tang, J., Baldocchi, D., Xu, L., 2005a. Tree photosynthesis modulates soil respiration on a diurnal time scale. Global Change Biology 11, 1298–1304.

Tang, J., Mission, L., Gershenson, A., Cheng, W., Goldstein, A., 2005b. Continuous measurements of soil respiration with and without roots in a ponderosa pine plantation in the Sierra Nevada Mountains. Agricultural and Forest Meteorology 132, 212–227.

Thompson, M., Holbrook, N., 2004. Scaling phloem transport: information transmission. Plant Cell and Environment 27, 509–519.

Urbanski, S., Barford, C., Wofsy, S., Kucharik, C., Pyle, E., Budney, J., McKain, K., Fitzjarrald, D., Czikowsky, M., Munger, J.W., 2007. Factors controlling CO_2 exchange on timescales from hourly to decadal at Harvard Forest. Journal of Geophysical Research 112, G02020.

Xu, M., Qi, Y., 2001. Spatial and seasonal variations of Q_{10} determined by soil respiration measurements at a Sierra Nevadan forest. Global Biogeochemical Cycles 15, 687–696.

Xu, L., Baldocchi, D., Tang, J., 2004. How soil moisture, rain pulses, and growth alter the response of ecosystem respiration to temperature. Global Biogeochemical Cycles 18, GB4002.

Yuste, J., Janssens, I., Carrara, A., Ceulemans, R., 2004. Annual Q_{10} of soil respiration reflects plant phonological patterns as well as temperature sensitivity. Global Change Biology 10, 161–169.